Fracture Mechanics of Concrete and Concrete Structures - Assessment, Durability, Monitoring and Retrofitting of Concrete Structures- B. H. Oh, et al. (eds)
© 2010 Korea Concrete Institute, Seoul, ISBN 978-89-5708-181-5

Study on the influencing factors of steel corrosion in cracked concrete

W. Tian, A. Volkwein & P. Schießl
Center for Building Materials, Technical University of Munich, Germany

ABSTRACT: The passive layer of embedded steel in concrete can be easily broken down by chloride ions. Hereby, when cracks occur, macro cell corrosion will be encouraged by making the migration of chloride possible. To investigate the corrosion process and dominant influencing factors, laboratory tests were carried out on central cracked beams, in which a corrosion system with single anode and multiple cathodes was well designed. The beams are subjected to both chloride/water wetting cycle and natural exposures. Corrosion currents and potential are selected to be the basic research parameters. Data from 20 months' daily measurement have been collected. Effects of concrete composition, exposure, cover depth, as well as carbonation are studied. It is also found out that the ratio of anode and cathode surface plays an important role in the distribution of corrosion currents.

1 GENERAL INSTRUCTIONS

1.1 *Cracked concrete*

Concrete is the most commonly used construction material nowadays. Sound concrete has superior properties in load bearing capacity and durability. However, this seemingly ideal material is not always crack free. Cracks in concrete can be caused by internal shrinking or external variation of environment (e.g. temperature). Loading is also a major inducement. Cracks in concrete accelerate the ingression of moisture and corrosion promoting substances, finally devastating its structural robustness. Considering the structures exposed to sea water and/or deicing salt, chloride penetration is a common cause of deterioration of reinforced concrete. So the German Research Foundation financed the research 'corrosion of steel in cracked concrete' as a subproject of the main project "Modeling of Reinforcement Corrosion".

1.2 *Electrolytic chemical model for corrosion in concrete*

An electrical circuit model can be used as physical model, Figure 1 and Equation 1. Thereby, the corrosion rate can be defined as the quotient of the driving potential and the sum of all system resistances.

$$I_{corr} = \frac{U_0}{\frac{r_a}{A_a} + \frac{r_c}{A_c} + \rho_e \cdot k_e} + I_{corr,0} \qquad (1)$$

with I_{corr} as total corrosion current in $[A]$, $I_{corr,0}$ as micro corrosion current in $[A]$, U_o as driving voltage in $[V]$, r_a and r_c as area specific polarisation resistances of anode and cathode in $[\Omega m^2]$, A_a and A_c as areas of anode and cathode in $[m^2]$, ρ_e as resistivity of concrete in $[\Omega m]$ and k_e as cell constant in $[m/m^2]$.

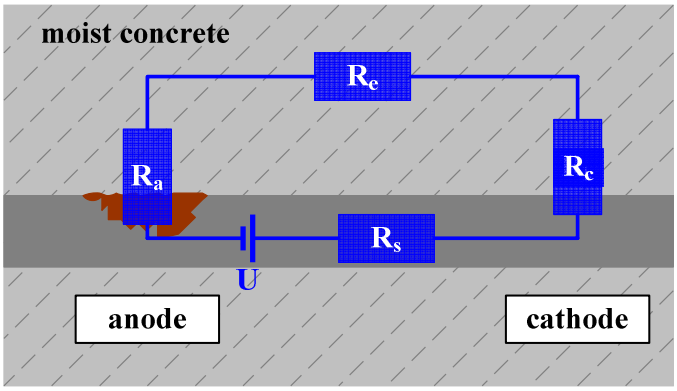

Figure 1. Electrical circuit model.

The increase of corrosion depth $\Delta x_{corr}(t)$ can be obtained by using the corrosion rate and Faradays law as shown in Equation 2.

$$\Delta x_{corr}(t) = \int_{\Delta t} \left(i_{corr}(t) \cdot \Delta t \cdot Y \right) \cdot dt \qquad (2)$$

Herein, $\Delta x_{corr}(t)$ is the increase of corrosion depth at a given time in $[m]$, $i_{corr}(t)$ is defined as the quotient of corrosion current I_{corr} and anodic area A_a in $[A/m^2]$, Δt as time in $[s]$ and Y constant which is $36.866 \cdot 10^{-12}$ $[m^3/C]$.

A first quantification of the main influences on the corrosion current I_{corr} has been done during the first period of funding of the research group DFG-FOR 537 for a homogeneous that means uncracked concrete (Schießl & Osterminski 2006, Beck et al. 2006, War-

kus & Raupach 2006, Osterminski et al. 2006, Büteführ et al. 2006, Bohner & Müller 2006).

2 EXPERIMENTAL

2.1 *Specimens*

In order to investigate the influence of cracks on the corrosion rate, a well defined crack orthogonal to the steel bar representing the anode had to be produced. For measuring the corrosion rate as electrical current separated cathodes had to be arranged near to the anode. A specimen design, cuboids with $500 \times 200 \times 150 mm^3$, has been developed allowing a predefined cracking in a tension test.

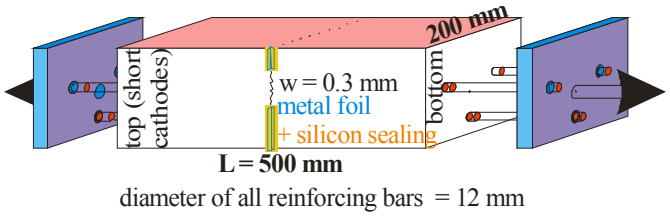

Figure 2. Geometry of cracked concrete beam.

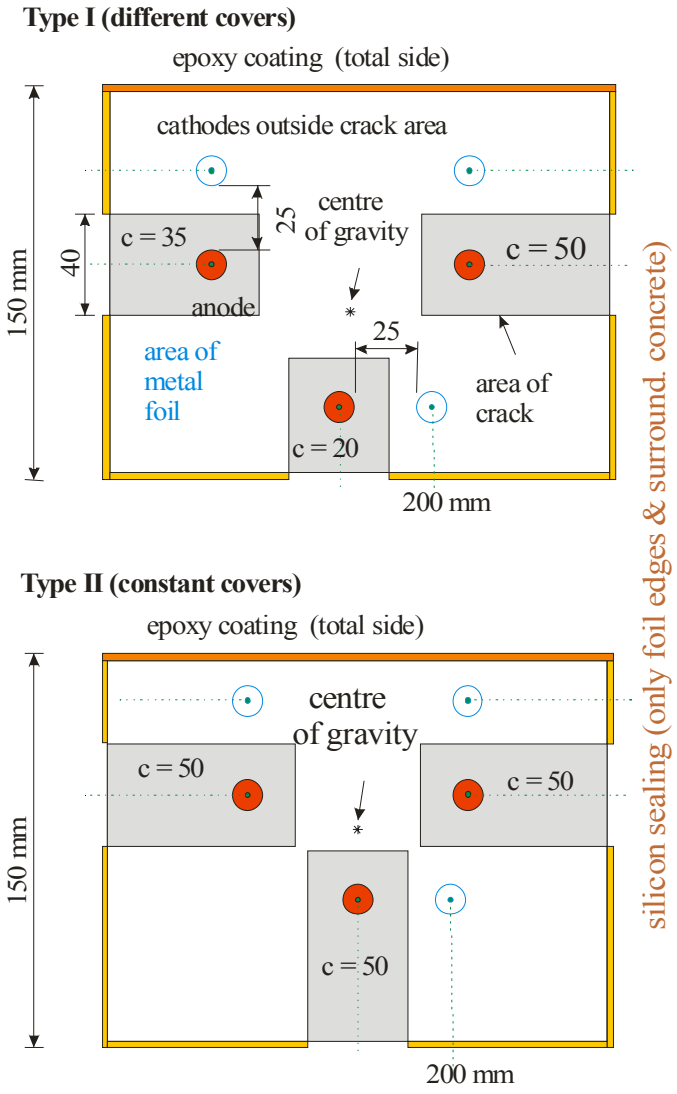

Figure 3. Cross section of cracked beams, Type I, different cover, Type II, constant cover.

Each specimen contains three bars (d = 12 mm) reaching from one end to the other and being coated with epoxy resin except a small anode area of 40 mm of length (Aa = 15.1 cm²). These bars are fixed in the mould with three different (20, 35 and 50 mm, Type I) or three equal (50 mm, Type II) cover depths. To be able to create a well defined crack in the middle of the beam length orthogonal to the bars double layered thin metal foils are located around the bars to weaken the cross section and form a predetermined crack area. In order to prevent water transport the two foils (stainless steel) were later glued together at their inner edges by using silicon. The ends of the bars are welded to steel plates which are provided with anchors for loading under tension. These anchors, the three steel bars and the concrete cross section formed by the metal foils are arranged around the same centre of gravity.

In parallel to each anode bar three short pieces (l = 50 mm) and one longer bar (l = 150 mm) of the same steel are arranged as cathodes without any electrical contact between them and the anodes. In addition, close to each anode area a reference electrode is fixed inside the mould for the potential measurements, Figure 4. Hence, a nearly IR-drop-free potential measurement of the anodes is possible.

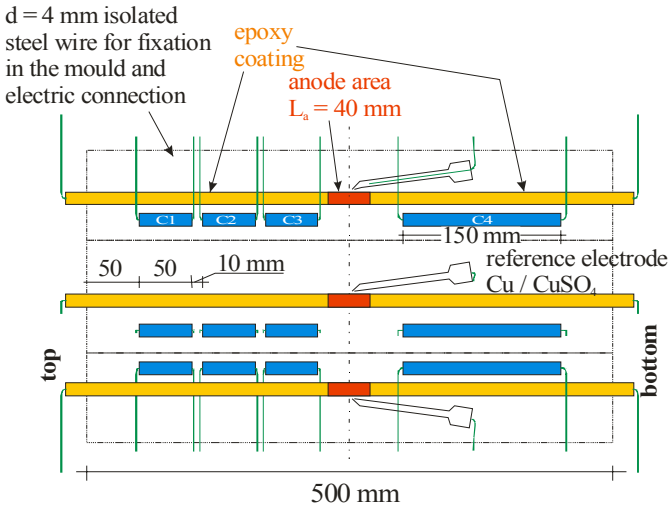

Figure 4. Scenograoh of corrosion system (cathodes C1-C3 with 50 mm length, C4 with 150 mm, and anode with 40 mm in the centre).

As cement type a Portland cement (CEM I 32.5 R) and a blast furnace slag cement (CEM III/A 32.5 N-LH) with a content of 360 kg/m³ were used. Furthermore limestone sand and gravel with a maximum aggregate size of 16 mm, tap water and water reducing agent at a w/c ratio of 0.50 and 0.40 respectively complete the concrete mixture. The mean value of the cube strength at an age of 28 days was about 40 N/mm². For curing, the specimens were left in the molding at 20°C and 85% relative humidity (RH) for 7 to 14 days. Afterwards the cracks were produced in a testing machine. The crack width was first adjusted to about 0.32 mm. Then metal foils of

0.30 mm thickness were inserted between the two embedded foils and the load was reduced again activating the spring force of the reinforcement. Hence, the crack width could be set precisely to 0.30 mm having it crossing exactly through the anodic area of the reinforcement. Afterwards, both steel plates were cut off.

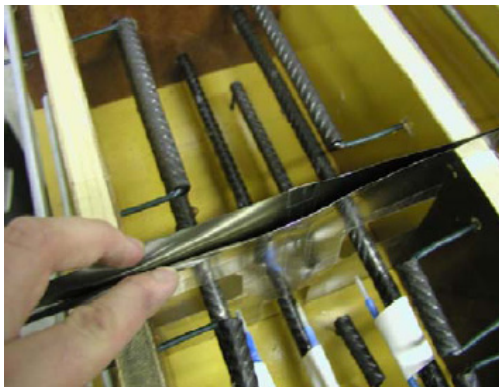

Figure 5. View into the prepared mould.

After these preparations the specimens were stored again in 20°C / 85% RH until hydration of the cements was proceeded to an age of about 180 days. During this period the concrete surface without exposure was coated by epoxy resin. The coating was necessary to comply with the aim of one dimensional influence on the cover of each anode and its corresponding cathodes.

2.2 *Measuring technique*

The corrosion current is measured once daily. Between these measurements the four cathodes and one anode are short circuited by a four-pole switch in 'stand by' position, Figure 6. The current is converted into a voltage by an inverting operational amplifier (zero-Ohm-measurement). Therefore, the measured values have to be inverted (multiplied by (-1)) to obtain the corrosion current. The reference voltage is measured by an amplifier with 100 MΩ input resistance. According to the anodic potential the measured voltage has to be inverted, too (Fig. 6). The measurement starts by connecting the amplifier box to the connection device. Afterwards the switch is opened and the measured voltages are logged. Before unplugging the amplifier box the switch has to be shortened again. Hereby, the corrosion process is hardly disturbed.

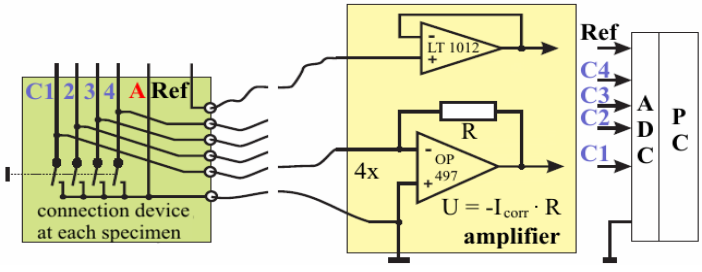

Figure 6. Electrical setup for measuring instruments.

2.3 *Exposure*

During exposure only anodes should be charged with water or chloride solution. A supply of oxygen at the cathodes can be provided by a more or less dry and exposure-free concrete surface. This setup allows a study of macro cell corrosion systems. The specimens are stored in an upright position with gutter glued around the concrete surface at the height of the cracks. Inside the gutter a hose with drill-holes is positioned. The gutter prevents leakage of water or chloride solution outside of crack areas which is sprayed out of the hose, Figure 7.

Three kinds of exposure are selected:

1 Chloride cycle: Similar to water cycle but spraying with salt solution instead of water (1.0 m.-% Cl^- by $NaCl : CaCl_2 = 9:1$),

2 Water cycle: Storage in the lab (≈20°C/≈65% RH) and wetting of the cracks is every week for one hour,

3 Outside (Munich, Germany): Subjected to normal weather conditions (direct rain, wind, sun etc.).

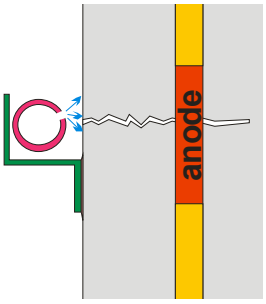

Figure 7. Wetting system.

In order to have the possibility to process a statistical analysis of the results an adequate amount of specimens was produced, see Table1.

Table 1. Layout of specimens in three exposures.

	Chloride cycle	Water cycle	Outside
CEM I 32.5R (w/c=0.5)	3/3	3/1	4/1
CEM III/A 32.5 R (w/c=0.5)	3/1	3/04/1	
CEM III/A 32.5 R (w/c=0.4)	0/1	0/00/0	

* Type I / Type II

* One carbonation specimen for each concrete composition in each exposure.

3 RESULTS

3.1 *Initiation period*

The passive film is a thin, sound layer which forms on the metal surface by anodic reaction. It separates the metal and the electrolyte hence protects metal from corrosion. However, it can be disrupted when

carbonation front reaches the steel or chloride content around the steel surface exceeds a certain value, the so called critical content or threshold value. The duration before the break down of this oxide layer is considered as the end of initiation period. Breakdown of passive film by chloride ions leads to localized corrosion which, compared to the relatively uniform corrosion caused by carbonation, induces greater cross section loss.

In the range of this research, depassivation is judged by the observation of a sudden drop in corrosion potential and the simultaneous strong increase in corrosion current, associated with the assumption that the whole anode area is completely depassivated ($A_a \approx 15.07 cm^2$).

As mentioned in chapter 2, corrosion current and potential are measured daily so that mountains of data have been collected.

After 20 months' storage in the three different exposures, most specimens in chloride cycle have shown active behavior; however, nearly no specimens in water cycle and the natural exposure have been depassivated. So the results presented in this paper are only focused on the samples which are subjected to chloride exposure. Results are obtained from adequate amount of specimens so that probabilistic analysis can be conducted as well.

3.2 *Effects of concrete cover*

Concrete cover provides protection to the embedded steels. Generally in sound concrete, the thicker and tighter the cover is, the better protection it offers. So an adequate concrete cover is commonly suggested by design codes.

Figure 8 contains information about cover depth effect on steel depassivation in cracked concretes. Anodes with 2 cm cover depth depassivated with an average duration of 53 days for CEM I concrete and 8 days for CEM III concrete. Initiation period reaches 120 days for CEM I concrete and 77 days for CEM III concrete when cover depth increases from 2 cm to 3.5 cm. But the thickest cover depth, 5 cm, didn't show superior ability in corrosion resistance.

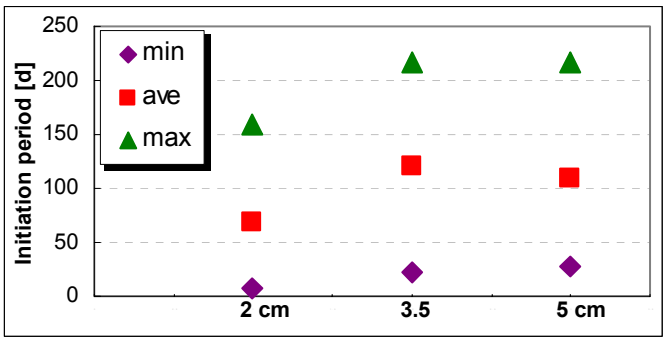

Figure 8 (a). Effect of concrete cover on initiation period, CEM I concrete, w/c ratio 0.5.

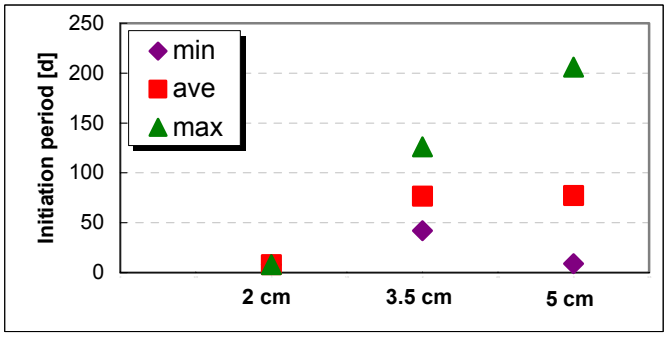

Figure 8 (b). Effect of concrete cover on initiation period, CEM III concrete, w/c ratio 0.5.

Although no clear influence of cover depth on depassivation can be observed in cracked concrete, a deeper concrete cover is still preferable, since it not only meet bearing capacity demands, but also closely related to crack frequency. The deeper the cover depth is, the lower the crack frequency will be, moreover, the amount of corrosion increases with crack frequency.

3.3 *Effect of concrete composition*

Figure 9 shows the influence of concrete composition on initiation period in a probabilistic way. With initiation period be the abscissa, the y-axis is the lognormal distribution density. As can bee seen in the diagram, the average initiation period for steels in CEM I concrete is 110 days, which is longer than that in CEM III concrete (77 days). Thereby cracked beams with CEM I concrete show a better resistance to chloride induced depassivation.

It is believed that only the chloride remaining in pore solution, the so called free chloride will break down the passive oxide layer and cause the corrosion of reinforcement. Researchers further pointed out that the Cl^- / OH^- ratio in pore solution influences the duration of initiation phase. Based on this knowledge, the result shown in Figure 9 seems to be a little bit controversial since CEM III concrete has a better chloride binding capacity than CEM I concrete. However, in the case of cracked beams, anode in cracked area is suffered from direct chloride solution spray; hence chloride content around anode is always sufficient enough for both cement type. So that influence of chloride binding capacity might not be as significant as in other cases. On the other hand, the Cl^- / OH^- ratio in CEMIII concrete might higher than the CEM I concrete due to a lower PH value. This gives the explanation that why the CEM III concrete behave actively earlier than CEM I concrete.

w/c ratio seems to play a crucial role in avoiding depassivation as well. Till now, all the three corrosion systems with a lower w/c ratio (w/c=0.4) still behave inactively, except that only one of them shows a sudden increase in corrosion current after

533 days wetting cycle, but in a relatively small range if compared with w/c ratio 0.5 specimens. Probabilistic analysis can not be done due to insufficient samples, so a density curve for w/c 0.4 samples is absent.

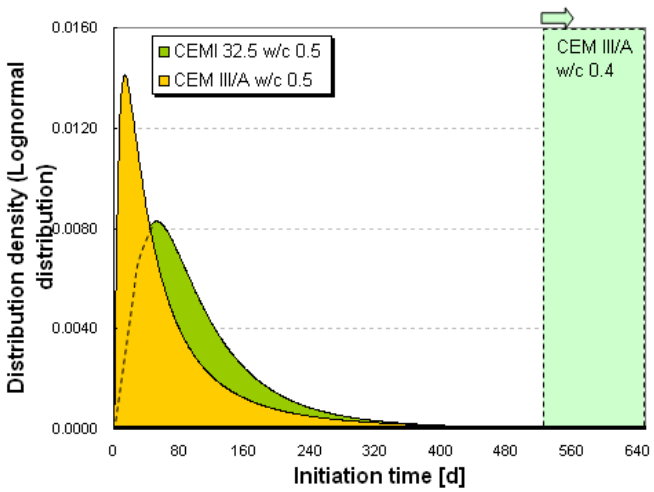

Figure 9. Distribution density curve of initiation period for CEM I concrete and CEM III concrete, c=5 cm.

3.4 *Corrosion current and potential*

After 20 months' cycling, nearly all the corrosion systems in chloride cycle with w/c ratio of 0.5 show active corrosion.

Figure 10 contains results of corrosion currents (a) and corrosion potentials (b) of selected active anodes. The three curves belong to corrosion systems from CEM I concrete with w/c ratio 0.5, CEM III concrete with w/c ratio 0.5, and CEM III concrete with w/c ratio 0.4 respectively. Each curve represents typical behaviour of its category. In the beginning, all the currents are around zero which indicates passive. After a few days exposure, the corrosion current in CEM I concrete increases steeply, which clearly announces the beginning of corrosion. It keeps on increasing till a peak of 250 µA was reached and then decreases gradually. According to the last measurements at 640 days, I_{corr} has dropped to 12µA. This might be because of the accumulation of corrosion products on the surface of anode hence the anodic oxidation is baffled, leading to repassivation again. Compared with CEM I concrete, corrosion in CEM III concrete is not so drastic. Corrosion current increases after depassivation and then decreases smoothly.

Although CEM I concrete has a better resistance for chloride induced depassivation, it can be observed in Figure 10 a (series 1 and 2) that once it depassivated, its corrosion is much intensive than CEM III concrete. This can be well explained by the results in parallelly conducted concrete electrolytic resistivity measurements in this research project, which indicates that resistivity of CEM I concrete is less than 2/5 of CEM III concrete.

The effect of w/c ratio should be noticed as well. As can be clearly seen in Figure 9, the corrosion currents in the concrete with a lower w/c ratio of 0.4 (CEM III) is nearly ignorable (series 3 in Fig. 10a). Meanwhile, the corresponding corrosion potential is also much higher than series 1 and series 2. If estimated by the judgement mentioned above, one can make the conclusion that the steel in this corrosion system is still passive. This can also be explained by the results from the concrete resistivity measurements which show that the resistivity of CEM III concrete with a w/c ratio of 0.4 is 1.4 times of that in CEM III concrete with a w/c ratio of 0.5, and 3.2 times of that in CEM I concrete with a w/c ratio of 0.5. The high resistance in low w/c ratio concrete successfully baffled the transportation of currents hence reduced corrosion. However, if zoomed in, a sudden rise from 0.1µA to 6µA in I_{corr} accompanied with a sudden drop in potential at 533 days can also be seen. Nevertheless, this can not be definitely considered as active or passive since the current is generally so small and meanwhile the anode area is still unknown.

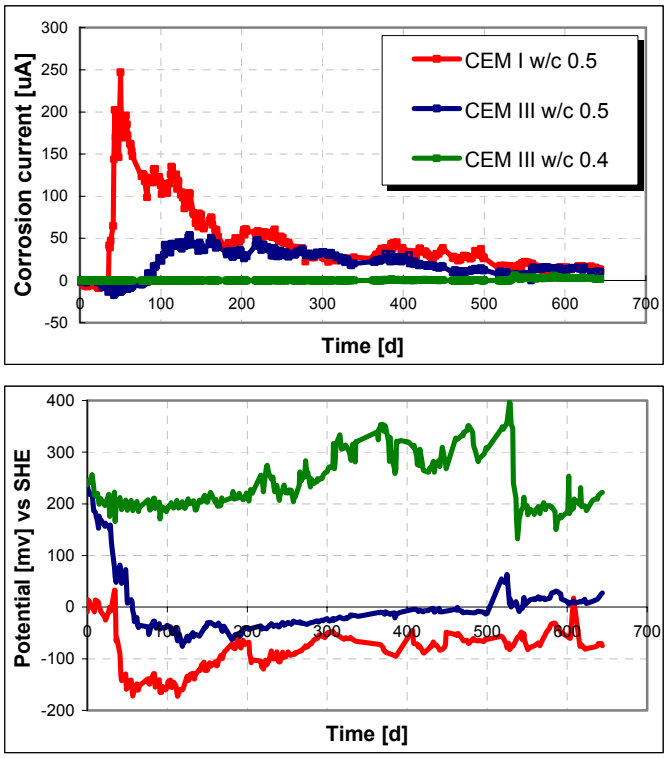

Figure 10. Summation of anodic corrosion currents of all cathodes (a); Anodic corrosion potential, c=5 cm (b).

As can be seen in Figure 10 b, development of potential with time shows a good agreement with corrosion current. A significant decrease of anode potential can be found after a few days exposure, accompanied by the steep increase of corrosion current in Figure 11 a. For the CEMI concrete sample, this potential drop ΔU is 0.16 V and in the case of CEM III concrete with w/c ratio 0.5, the potential drop

reaches 0.25 V, which leads to the simultaneous increase of I_{corr}.

Figure 11 give a general situation of the calculated mass loss of anodes with variable cover depth and different cement type, as well as carbonation state. Mass loss is calculated by Faraday's law with the following equation:

$$m = \frac{MI_{corr}\Delta t}{Fn} \quad (3)$$

where, m = mass loss in [g], M = the atomic mass of Fe (56 g/mol), I_{corr} = Corrosion current in [A], Δt = test period in [s], F = Faraday's constant, which equals to 96485.3383 C/mol. The carbonated specimens (only carbonated in the crack area for 0.5 mm's depth), which simulate the relatively older concrete structures, seem more susceptible than uncarbonated ones: an average magnify factor of 1.4 in mass loss can be found. In addition, for both CEM I concrete and CEM III concrete, a tendency of an increasing mass loss with increasing cover depth can be found. An explanation for this might be on one hand that cracks with deeper cover depth keep more moisture and higher chloride concentration after wetting, whereas cracks with smaller depth evaporate faster; On the other hand, oxygen in deeper cracks is relatively sparse. Any way, this result needs further examination. A subsequent experiment is being prepared. Results of mass loss will be validated after specimen opening as well.

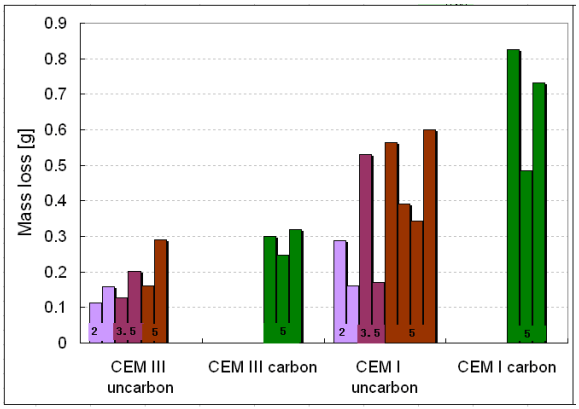

Figure 11. Mass loss, samples with w/c ratio 0.5.

3.5 *Corrosion current distribution among cathodes*

As introduced in Chapter 2.2, in one corrosion system (1 anode and 4 cathodes), the corrosion currents in different cathodes are measured separately. So their participation in the corrosion process can be observed.

Figure 12 shows the distribution of corrosion currents among the four cathodes. Data are collected from 7 corrosion systems with 5 cm cover depth. One can find that the distant cathodes, C1 and C2 only seize a quite small proportion of the total corrosion currents. The closest cathodes, C3 and C4, receive nearly 80% of the whole corrosion current. The cathodes which has the largest size, C4 (15 cm long), share more than half of the corrosion current. This diagram clearly indicates that distance between anode and cathode, as well as cathode surface significantly influence the corrosion current distribution.

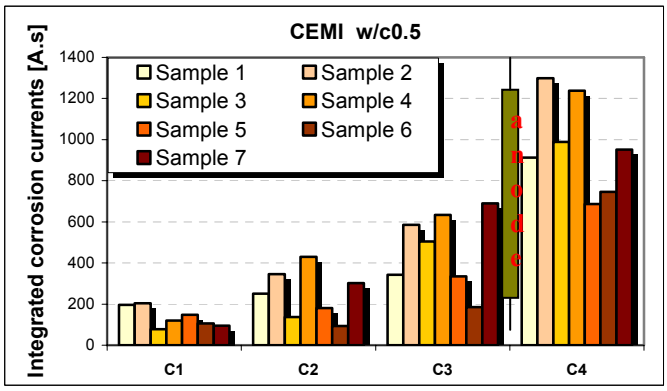

Figure 12. Distribution of corrosion currents among cathodes (c=5 cm).

4 CONCLUSIONS

In order to investigate the influencing factors on corrosion of steel in cracked concrete, a well designed corrosion system in central cracked concrete beam is introduced. Effects of factors, e.g. cement type, w/c ratio, concrete cover, exposure as well as carbonation on the corrosion process are analyzed. Based on the results, the following conclusions can be obtained:

- The corrosion system presented in this paper can be considered as an electrolyte-resistance-governed system since the conditions needed for anodic and cathodic reaction can be well fulfilled. Thereby factors such as cement type and w/c ratio which essentially influence concrete resistivity have the most crucial effects on both initiation period and propagation period.
- The influence of cover depth on corrosion process in crack concrete is not obvious at least in the range of this paper.
- Compared to uncarbonated concrete, carbonated concrete seems to be more susceptible to chloride induced corrosion.
- Distance between cathode and anode, as well as cathode/anode ratio significantly influence the participation of cathodes in the corrosion process.

ACKNOLEDGEMENT

Subproject A3 is part of the DFG research group 537 "Modelling Reinforcement Corrosion". The authors

wish to thank the German Research Foundation (DFG) for supporting this project.

* The description of the experimental setup and electrolytic chemical model have been published in 2008, Icorrr, South Africa, by K Osterminski (see reference).

REFERENCE

A. Arya &F.K. Ofori-Darko, Influence of crack frequency on reinforcement corrosion in concrete. Cement and Concrete Research, Vol.26, No. 3, pp.345-353,1996

C. Arya & J.B. Newman, Problem of predicting risk of corrosion of steel in chloride contaminated concrete, Proc. Instn. Civ. Engrs, Part 1, 88,875,1990

Beck, M.et al. 2006. Modelling of reinforcement corrosion - Influence of concrete technology on corrosion development. Materials and Corrosion, Vol. 57, 2006(12), pp. 914-919.

Bohner, E.& Müller, H.S. 2006. Modelling of reinforcement corrosion - Investigations on the influence of shrinkage and creep on the development of concrete cracking in the early propagation stage of reinforcement corrosion. Materials and Corrosion, Vol. 57, 2006(12), pp. 940-944.

Büteführ, M et al. 2006. On-site investigations on concrete resistivity - a parameter of durability calculation of reinforced concrete structures. Materials and Corrosion, Vol. 57, 2006(12), pp. 932-939.

Osterminski, K et al. 2006. Modelling reinforcement corrosion - usability of a factorial approach for modelling resistivity of concrete. Materials and Corrosion, Vol. 57, 2006(12), pp. 926-931.

Osterminski, K et al.: DFG-Research Group 537: Modelling of Reinforcement Corrosion – Corrosion Measurements on Cracked Reinforced Concrete Beams. Proceedings: ICCRRR 2008, Cape Town.

Schießl, P & Osterminski K. 2006. DFG-research-group: Modelling reinforcement corrosion - overview of the project. Materials and Corrosion, Vol. 57, 2006(12), pp. 911-913

Warkus. J.& Raupach, M. 2006. Modelling of reinforcement corrosion - Corrosion with extensive cathodes. Materials and Corrosion, Vol. 57, 2006(12), pp. 920-925.